COMPUTATIONAL STRATEGIES IN OPTIMIZING A REAL-TIME GRAD-SHAFRANOV PDE SOLVER USING HIGH-LEVEL GRAPHICAL PROGRAMMING AND COTS TECHNOLOGY

L. Giannone*, R. Fischer, K. Lackner and ASDEX Upgrade Team

Max-Planck Institut für Plasmaphysik, EURATOM-IPP Association, D-85748 Garching, Germany

P.J. McCarthy

Department of Physics, University College Cork, Cork, Ireland

Q. Ruan, A. Veeramani, M. Cerna, J. Nagle, M. Ravindran, D. Schmidt, A. Vrancic, L. Wenzel

National Instruments, Austin, TX 78759-3504, Texas, USA

Abstract

Big physics control experiments require enormous computational power to solve large problems with demanding real-time constraints. Sensors are acquired in real-time to feed mathematical routines, which then generate control outputs to real-world processes. For tokamak control, a non-linear PDE needs to be solved in real-time with a cycle time of less than 1 ms.

We report on an alternative approach based on LabVIEW that solves the critical plasma shape and position control problems in tokamaks. Input signals from magnetic probes and flux loops are the constraints for a non-linear Grad-Shafranov PDE solver to calculate the magnetic equilibrium. An architecture based on off-the-shelf multi-core hardware and graphical software is described with an emphasis on seamless deployment from development system to real-time target. A number of mathematical challenges were addressed and several generally applicable numerical and mathematical strategies were developed to achieve the timing goals. Several benchmarks illustrate what can be achieved with such an approach.

INTRODUCTION

The magnetic equilibrium for a tokamak is described by the Grad-Shafranov equation :

$$R\frac{\partial}{\partial R}\left(\frac{1}{R}\frac{\partial\psi}{\partial R}\right) + \frac{\partial^2\psi}{\partial Z^2} = -\mu_0 R\mathbf{j}(R, Z), \quad (1)$$

where ψ is the poloidal flux function, $\mathbf{j}$ is the current density, R is the radial component and Z is the axial component (see figure 1). This problem is commonly solved by a cyclic reduction algorithm [1, 2, 3]. A magnetic equilibrium for discharges with plasma current is reconstructed on a 33 x 65 grid using 40 magnetic probes and 18 flux loop difference signals. The right hand side current density term is calculated by a weighted least squares fit to the measurements which yields coefficients for the basis current density profiles [2, 3, 4]. Three basis current density profiles were chosen in the first round of development and found to adequately fit the experimental magnetic probe

---

*Louis.Giannone@ipp.mpg.de

and flux loop measurements [5]. The currents from the poloidal field coils are also needed to compute the value of ψ on the spatial grid.
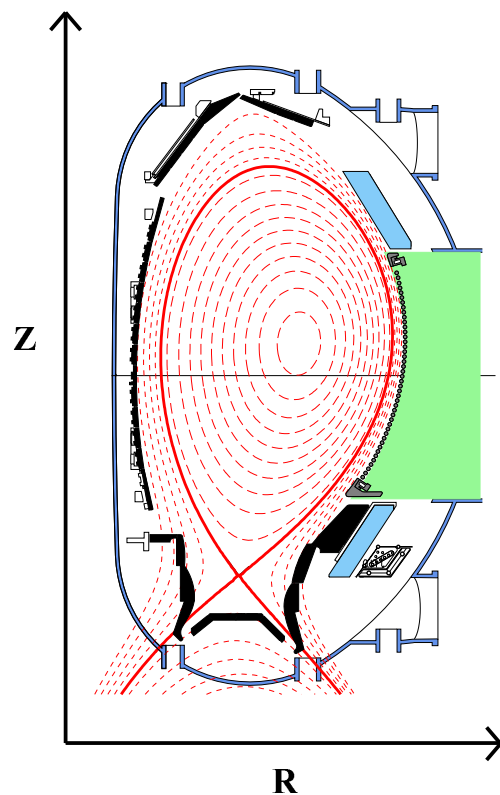

Figure 1: The cross section of the ASDEX Upgrade tokamak showing the flux surfaces of the magnetic equilibrium (red dotted lines) and plasma separatrix (red solid line).

REAL TIME GRAD-SHAFRANOV SOLVER

We report on a new spectral-based algorithm to solve the Grad-Shafranov equation in an unbounded domain. The new algorithm adapts a method commonly used to solve the Poisson equation in cylindrical coordinates. The use of discrete sine transforms (DST) along the Z-axis and a

tridiagonal solver [6, 7] is an alternative to the cyclic reduction algorithm to solve the Grad-Shafranov equation for poloidal flux, ψ.

Spectral Method

A uniform mesh with constant spacing dR and dZ in the R and Z directions is assumed. The grid points are labeled from 0 to $NZ-1$ and 0 to $NR-1$, where NZ is the number of grid points in the Z direction, and NR is the number of points in the R direction. The five point difference equation with index i in the R direction and index j in the Z direction can be written as :

$$\frac{\psi_{i+1,j} - 2\psi_{i,j} + \psi_{i-1,j}}{dR^2} - \frac{1}{R_i}\frac{\psi_{i+1,j} - \psi_{i-1,j}}{2dR}$$
$$+ \frac{\psi_{i,j+1} - 2\psi_{i,j} + \psi_{i,j-1}}{dZ^2} = -\mu_o R_i \mathbf{j}_{i,j} \quad (2)$$

Introducing the discrete sine transform of ψ and $\mathbf{j}$:

$$\phi_{i,k} = \sum_{j=1}^{NZ-2} \psi_{i,j} sin\left(\frac{\pi jk}{NZ-1}\right) \quad (3)$$

$$J_{i,k} = \sum_{j=1}^{NZ-2} \mathbf{j}_{i,j} sin\left(\frac{\pi jk}{NZ-1}\right) \quad (4)$$

leads to the tridiagonal matrix equations :

$$\beta_i\phi_{i+1,k} - \alpha_k\phi_{i,k} + \gamma_i\phi_{i-1,k} = -\mu_0 R_i dR^2 J_{i,k} \quad (5)$$

where $\alpha_k = 2 + 4S^2 sin^2\left(\frac{\pi k}{2(NZ-1)}\right)$, $\beta_i = 1 - dR/(2R_i)$, $\gamma_i = 1 + dR/(2R_i)$ and $S = dR/dZ$.

Tridiagonal Solver

The tridiagonal matrix equation is solved with a tridiagonal solver using an LU decomposition algorithm. The LU decomposition generates two bidiagonal matrices subsequently used in the iterative procedure to solve the tridiagonal equations. By using LU decomposition, operations are reduced by a factor of 2 compared to the direct solver algorithm [8].

Unbounded Domain

The solver for the Grad-Shafranov equation in an unbounded domain is composed of two fast solver steps [1]. The new algorithm reduces the computing time dramatically by utilizing a spectral method at each step.

The first step of the solver uses zero as the condition for all grid boundaries with a right hand side current distribution on the flux surfaces from the previous iteration given by the weighted least squares fit to the magnetic probe and flux loop measurements. In this step, it is only necessary to compute ψ at points neighboring the grid boundary and

a reduced inverse DST can be performed to calculate these values. The columns of ψ inside the boundary edge are :

$$\psi_{i,k} = \frac{2}{NZ-1}\sum_{j=1}^{NZ-2}\phi_{i,j}sin\left(\frac{\pi jk}{NZ-1}\right) \quad (6)$$

where $i = 1$ and $NR - 2$, and the rows inside the boundary edge can be calculated in a similar fashion with $k = 1$ and $NZ - 2$. All these four edges can be computed using matrix-vector multiplication. This avoids the unnecessary computations performed by a traditional inverse DST operation applied to the entire grid. The gradients in ψ normal to the grid boundary, $(\partial\psi/\partial n)_{boundary}$, are the inputs required for the next solver step. These are the shielding currents that are necessary to force the zero boundary condition of the first solver step. They are used to calculate the Green's functions for ψ generated by a current hoop of radius, a, carrying current, I, for each grid point with radial coordinate, R, and a vertical distance, Z, on the boundary [1, 9, 10] :

$$\psi = \mu_o I\sqrt{(a+R)^2 + Z^2}((1-k^2/2)K(k^2) - E(k^2)) \quad (7)$$

where $k^2 = 4aR/((a+R)^2 + Z^2))$, $K(k^2)$ is the complete elliptic integral of the first kind and $E(k^2)$ is the complete elliptic integral of the second kind [11, 12]. The actual calculation of the resulting ψ on the boundary is performed as a matrix multiplication with pre-calculated coefficients times the vector of shielding currents.

The second step of the solver is carried out with boundary conditions from the first solver step but without current source terms on the right hand side of the Grad-Shafranov equation. Because only the first and last elements are nonzero, it is possible to use an optimized DST to reduce the computation effort. The faster DST is carried out by the BLAS function *dger* producing :

$$D_{ij} = -\frac{\psi_{i,1}sin\left(\frac{\pi j}{NZ-1}\right) + \psi_{i,NZ-2}sin\left(\frac{\pi j(NZ-2)}{NZ-1}\right)}{dZ^2}$$
$$= -\frac{\psi_{i,1} - (-1)^j\psi_{i,NZ-2}}{dZ^2}sin\left(\frac{\pi j}{NZ-1}\right) \quad (8)$$

The DST of the boundary conditions at the inner and outer radial positions are added to the first and last columns. The tridiagonal solver is applied to this result and is added to the result from the first solver step. The solution of the Grad-Shafranov equation is then calculated by an inverse DST.

Under equivalent boundary conditions, an implementation based on the cyclic reduction algorithm computes all elements on the grid in both solver steps. The Grad-Shafranov solver algorithm described here achieves a significant performance improvement in comparison to cyclic reduction by employing two optimized DST implementations. The first implementation exploits the ability to avoid unnecessary calculations. The second implementation exploits the fact that the right hand side term is zero except at the boundary to greatly reduce the number of operations.

The ψ generated by the external poloidal field coils and passive stabilizing loop on the grid is also realized as a matrix-vector multiplication using factors calculated with Equation 7. The poloidal field coils and passive stabilizing loop are simulated as a finite number of filaments, with each filament carrying an applicable number of turns. Vacuum field shots with current pulses successively in each of the poloidal field coils are carried out to ensure that the best possible estimates of the magnetic probe and flux loop positions and calibration factors of the integrators are used to reconstruct the tokamak magnetic equilibrium with plasma current [5].

BENCHMARKS

A Dell T5500 with two PCI-e x16 slots wired as x8 (half length), two PCI-e x16 Gen 2 graphics slots up to 150 watts each, a PCI-X 64bit/100MHz slot with support for 3.3V or universal cards (half length) and a PCI 32bit/33MHz 5V slot (half length in desktop orientation) has been delivered with LabVIEW RT 2009 installed. A dual port Gigabit Ethernet card, a x4 PCIe VMIC 5565 PIORC reflective memory card and a NI PCIe 8362 interface card for connection of 2 PXI 1045 chassis for data acquisition of up to 256 channels were installed. Floating point benchmarks indicate a factor of up to 2.7 increase in performance in comparison to the current dual quad-core 3 GHz Xeon 5365 computer currently used for data acquisition and real-time calculations of magnetic equilibrium using only function parameterization [13]. The reflective memory card transmits the 33x65 poloidal flux matrix value to the control system with less than 1 ms delay. A third party PCI card delivers 64 bit time stamps using a 100 MHz clock and generates the 10 MHz TTL pulses for clock synchronization of the data acquisition boards in a number of data acquisition systems.

The following cycle time benchmarks were achieved for the real time Grad-Shafranov solver (GS) :

Table 1: Benchmarks for a single iteration of the real-time Grad-Shafranov solver (GS) using 8 CPU cores and LabVIEW RT 2009.

Platform	GS (ms)
Xeon X5365 @ 3.0 GHz	1.13
Xeon X5677 @ 3.46 GHz	0.63

The achieved cycle time for the Grad-Shafranov solver is therefore satisfactory for the real-time processing requirements of neoclassical tearing mode stabilization experiments where the cycle time of the discharge control system is 1.3 ms [14]. It should be noted that these benchmarks are for a single cycle iteration for the PDE solution. A detailed comparison of real-time magnetic equilibrium reconstruction with well converged solutions from offline calculations show that the small differences that are found for relatively

steady state conditions are not relevant for practical discharge control [2].

CONCLUSION

A real-time Grad-Shafranov solver based on a discrete sine transformation of the difference equation rather than cyclic reduction has been realized. The resulting tridiagonal equations are solved with a specially developed subroutine based on LU factorization. This tridiagonal solver reduces the number of operations with respect to the iterative direct solver by pre-calculating the reciprocal of the diagonal elements. A reduced inverse DST is required in the first solver step as only the relevant terms for those neighbors of the grid boundary need be calculated. A simplified DST can used for the second solver step where only the first and last elements are non-zero. In this way the full inverse DST of the first solver step is omitted and the DST of the second solver step without current source terms can be calculated with a smaller number of operations. The real-time Grad-Shafranov solver cycle time of 0.63 ms on the delivered Dell T5500 platform satisfies the ASDEX Upgrade real-time processing requirements.

REFERENCES

[1] K.Lackner, Comp. Phys. Comm., **12**, 33 (1976)

[2] J.R.Ferron, M.L.Walker, L.L.Lao et. al, Nuc. Fusion **36**, 1055 (1998)

[3] P.J. McCarthy, Physics of Plasmas, **6**, 3554 (1999)

[4] W.Zwingmann et. al, Plasma Phys. Control. Fusion, **43**, 1441 (2001)

[5] L.Giannone, R.Fischer, J.C.Fuchs et. al, http://ocs.ciemat.es/EPS2010PAP/pdf/P4.122.pdf

[6] R.W.Hockney and J.W.Eastwood, "Computer simulation using particles", p208, Taylor and Francis (1988)

[7] M.H.Hughes, Comp. Phys. Comm., **2**, 157 (1971)

[8] W.H.Press, S.A.Teukolsky, W.T.Vetterling and B.P.Flannery, "Numerical Recipes in C", p50, Cambridge University Press, (1999)

[9] J.D.Jackson, "Classical Electrodynamics", p142, Wiley, (1999)

[10] J.Simpson, J.Lane, C.Immer and R. Youngquist, Simple analytic expressions for the magnetic field of a circular current loop http://ntrs.nasa.gov/archive/nasa/casi.ntrs.nasa.gov/20010038492001057024.pdf

[11] M.Abramowitz and I.A.Stegun, "Handbook of Mathematical Functions", p591, National Bureau of Standards (1972)

[12] M.Abramowitz and I.A.Stegun, "Handbook of Mathematical Functions", p588, National Bureau of Standards (1972)

[13] L.Giannone, W.Schneider, P.J.McCarthy et. al, Fusion Eng. Des. (2008), http://dx.doi.org/10.1016/j.fusengdes.2008.12.059

[14] W.Treutterer, L.Giannone, K.Lüddecke et. al, Fusion Eng. Des. (2008) http://dx.doi.org/10.1016/j.fusengdes.2008.12.026